Corrosion Inhibition Effect of N, N'-diphenylthiourea on the Electrochemical Characteristics of Mild steel in Dilute Acidic Environments

[1, 2]Roland Tolulope Loto*, [1, 2]Cleophas Akintoye Loto, [2]Abimbola Patricia Popoola and [3]William Kupolati
[1]*Department of Mechanical Engineering, Covenant University, Ota, Ogun State, Nigeria.*
[2]*Department of Chemical, Metallurgical and Materials Engineering, Tshwane University of Technology, Pretoria, South Africa.*
[3]*Department of Civil Engineering, Tshwane University of Technology, Pretoria, South Africa.*
tolu.loto@gmail.com*

(Received on 14th July 2015, accepted in revised form 1st December 2015)

Summary: The electrochemical corrosion behaviour of n, n'-diphenylthiourea on the surface properties mild steel in attenuated sulphuric and hydrochloric acids (3M concentration) contaminated with 3.5% recrystalized sodium chloride at ambient temperatures was examined through weight loss analysis, open circuit potential monitoring and potentiodynamic polarization. The surface morphology of the samples was analyzed with scanning electron microscopy and x-ray diffractometry. Statistical analysis of the results was done with aid of ANOVA software to assess their statistical relevance. Results show the thiourea derivative performed more excellently in sulphuric than hydrochloric acid based on inhibition efficiency values. Observations from SEM/XRD image and data further confirm the results of experimental data. Statistical derivations reveal the overwhelming influence of exposure time on inhibition performance compared to concentration of the organic compound.

Keywords: Corrosion; Inhibitor; Acid; Steel; Adsorption.

Introduction

Mild steel is a ductile and weldable alloy accounting for over 80% of the annual steel production worldwide. It is extensively applied in industrial processing machinery and equipment in industries which includes petroleum and gas, minerals, fertilizers, marine applications, chemical processing, construction and metal-processing and semiconductor plants. However, the steel is highly vulnerable to corrosion, which occurs when applied in contact with corrosive solutions [1–3]. Initiation of the corrosion process results in the accumulation of corrosion products on the steel surface which eventually leads to secondary damage. Mitigation against corrosion can be achieved through assessment of various processes among which involves the application of corrosion inhibitors [4–7]. Corrosion protection of metals with the use of corrosion inhibitors, in a corrosive system at appropriate concentration, reduces the corrosion rate of the metals without particularly influencing the concentration of any of the corrosive reagents" has been known from historic times [8]. The aggressiveness and electrolytic characteristics of acidic conditions existing in industries necessitates the use of inhibitors, a cost effective method against steel corrosion. Organic compounds and their derivatives consists of heteroatoms such as oxygen, phosphorus, sulphur and functional groups multiple bonds within their molecule has been shown to give better inhibition performance compared to those containing nitrogen or sulphur only [9, 10]. Organic derivatives consisting of sulfur, nitrogen etc. with specific substituents is effective corrosion inhibiting compounds. Their inhibiting action can be deduced based on the number of available electron pairs, pi-orbital behaviour of available electrons and the electron density around the heteroatom [11–16]. N, N diphenylthiourea and its derivative have been used in previous research with excellent results [17-19]. This investigation aims to study the corrosion inhibiting performance and adsorption of n, n'-diphenylthiourea on the electrochemical characteristics ofmild steel in dilute sulphuric and hydrochloric acid solutions at surrounding temperature of 25 ^{o}C.

Experimental

Material

The mild steel used for this work was obtained in the open market and analyzed at the Applied Microscopy and Triboelectrochemical Research Laboratory, Department of Chemical and Metallurgical Engineering, Tshwane University of Technology, South Africa. The mild steel has the nominal per cent composition: 0.401C, 0.169Si, 0.440Mn, 0.005P, 0.012S, 0.080Cu, 0.008Ni, 0.025Al, and the rest being Fe.

*To whom all correspondence should be addressed.

Inhibitor

N, N-Diphenylthiourea (NNDT) a solid white powder is the inhibitor used. The structural formula of NNDT is shown in Fig. 1. The molecular formula is C_{13} H_{12} N_2 S, while the molar mass is 228.312 g mol^{-1}.

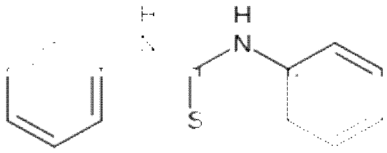

Fig. 1: Chemical structure of N, N-Diphenyl-thiourea (NNDT).

NNDT was prepared in concentrations of 0.25%, 0.5%, 0.75%, 1%, 1.25% and 1.5% per 200 ml of the acid media.

Test Media

0.5M sulphuric acid and 0.5M hydrochloric acid of 200 ml per concentration of NNDT each with 3.5% recrystallised sodium chloride of analar grade were used as the corrosion test media.

Preparation of Test Specimens

A cylindrical mild steel rod with a diameter of 14.5 mm was carefully machined and cut into a number of test specimens of average dimensions in length of 6 mm. A 3 mm hole was drilled at the centre for suspension. The steel specimens were then thoroughly rinsed with distilled water and cleansed with acetone for weight loss analysis. Linear polarization technique involved grinding the two surface ends of each specimen with silicon carbide abrasive papers of 80, 120, 220, 800 and 1000 grits before being polished with 6.0 μm to 1.0 μm diamond paste, washed with distilled water, rinsed with acetone, dried and stored in a dessicator before the test.

Weight-Loss Experiments

Weighted test species were fully and separately immersed in 200ml of the test media at specific concentrations of the NNDT for 432 h at ambient temperature. Each of the test specimens was taken out every 72 h, washed with distilled water, rinsed with acetone, dried and re-weighed. Plots of percentage inhibition efficiency (% *IE*) (calculated) versus exposure time (h) and percentage NNDT concentration (Fig. 4, 5, 8 and 9) were made from Tables (1 and 2).

The corrosion rate (R) calculation is from equation 1:

$$R = \left[\frac{87.6W}{DAT}\right] \quad (1)$$

where W is the weight loss in milligrams, D is the density in g/cm^2, A is the area in cm^2, and T is the time of exposure in hours. The %*IE* was calculated from the relationship in equation 2.

$$\%\ IE = \left[\frac{W1 - W2}{W1}\right] \times 100 \quad (2)$$

W_1 and W_2 are the weight loss in the absence and presence of predetermined concentrations of NNDT. The % *IE* was calculated for all the inhibitors every 72 h during the course of the experiment, while the surface coverage is calculated from the relationship:

$$\theta = \left[1 - \frac{W2}{W1}\right] \quad (3)$$

where θ is the substance amount of adsorbate adsorbed per gram (or kg) of the adsorbent. W_1 and W_2 are the weight loss of mild steel coupon in free and inhibited acid chloride solutions respectively.

Open Circuit Potential Measurement

A two-electrode electrochemical cell with a silver/silver chloride was used as reference electrode. The measurements of OCP were obtained with Autolab PGSTAT 30 ECO CHIMIE potentiostat. Resin mounted test electrodes/specimens with exposed surface of 165 mm^2 were fully and separately immersed in 200 ml of the test media (acid chloride) at specific concentrations of NNDT for a total of 288 h. The potential of each of the test electrodes was measured every 48 h. Plots of potential (mV) versus immersion time (hrs) (Fig. 6 and 7) for the two test media were made from the tabulated values in Tables (3 and 4).

Linear Polarization Resistance

Linear polarization measurements were carried out using, a cylindrical coupon embedded in resin plastic mounts with exposed surface of 165 mm^2. The electrode was polished with different

grades of silicon carbide paper, polished to 6 μm, rinsed by distilled water and dried with acetone. The studies were performed at ambient temperature with Autolab PGSTAT 30 ECO CHIMIE potentiostat and electrode cell containing 200 ml of electrolyte, with and without the inhibitor. A graphite rod was used as the auxiliary electrode and silver chloride electrode (SCE) was used as the reference electrode. The steady state open circuit potential (OCP) was noted. The potentiodynamic studies were then made from -1.5V *versus* OCP to +1.5 V *versus* OCP at a scan rate of 0.00166 V/s and the corrosion currents were registered. The electrochemical variables such as, corrosion potential (E_{corr}), corrosion current (i_{corr}) corrosion current density (I_{corr}), cathodic Tafel constant (*bc*), anodic Tafel slope (*ba*) , surface coverage θ and percentage inhibition efficiency (% *IE*) were calculated and given in Tables 3 and 4. The corrosion current density (I_{corr}) and corrosion potential (E_{corr}) were determined by the intersection of the extrapolating anodic and cathodic Tafel lines.

The corrosion rate (*R*), the degree of surface coverage (θ) and the percentage inhibition efficiency (% *IE*) were calculated as follows

$$R = \frac{0.00327 \times i_{corr} \times E_q}{D} \quad (4)$$

where i_{corr} is the current density in μA/cm^2, *D* is the density in g/cm^3; *E*q is the specimen equivalent weight in grams.The percentage inhibition efficiency (% *IE*) was calculated from corrosion current density values using the equation.

$$\% IE = 1 - \left[\frac{R_2}{R_1}\right] \times 100 \quad (5)$$

$R_1$and R_2 are the corrosion current densities in absence and presence of NNDT respectively.

Scanning Electron Microscopy Characterization

The surface morphology of the uninhibited and inhibited steel specimens were investigated after weight-loss analysis in 0.5 M H_2SO_4 and 0.5 M HCl solutions using Jeol scanning electron microscope for which SEM micrographs were recorded.

X-Ray Diffraction Analysis

X-ray diffraction (XRD) patterns of the film formed on the metal surface with and without NNDT addition were analyzed using a Bruker AXS D2 phaser desktop powder diffractometer with monochromatic Cu Kα radiation produced at 30 kV and 10 mA, with a step size of 0.03^o 2θ. The Measurement program is the general scan xcelerator.

Statistical Analysis

Two-factor single level statistical analysis using ANOVA test (F-test) was performed so as to investigate the significant effect of inhibitor concentration and exposure time on the inhibition efficiency values of the NNDT in the acid media.

The Sum of squares among columns (exposure time) was obtained with the following equations.

$$SS_c = \sum \frac{T_c^2}{nr} - \frac{T^2}{N} \quad (6)$$

Sum of Squares among rows (inhibitor concentration)

$$SS_r = \sum \frac{T_r^2}{nc} - \frac{T^2}{N} \quad (7)$$

Total Sum of Squares

$$SS_{Total} = \sum x^2 - \frac{T^2}{N} \quad (8)$$

Results and Discussion

Weight-loss Analysis

Weight-loss of the steel samples at specific time variation was evaluated with and without NNDT inhibitor addition in 0.5M H_2SO_4 and HCl acids respectively. Data obtained for the calculation of weight-loss (*W*), corrosion rate (*R*) and the percentage inhibition efficiency (% *IE*) values are depicted in Tables-1 and 2. Fig. 2 and 4 shows the plots of percentage inhibition efficiency against exposure time at predetermined concentrations of NNDT while Fig. 3 and 5 displays the plots of % *IE* versus inhibitor concentration. The loops obtained in Fig. 3 decreased sharply at 0.75% NNDT from high % *IE* values to lower values as NNDT concentration increases. After 0.75% NNDT inhibitor concentration, a progressive increase in % *IE* occurred till 1.5% NNDT. At 0.25% - 0.5% NNDT concentration the % *IE* value is above 90% as a result of its molecular structure, functional groups and the electrochemical interaction of its heteroatoms with the steel at the metal/solution interface. The steel surface passivates with increase in NNDT concentration due to increase in the number of interacting inhibitor molecules.

Table-1: Corrosion data for weight-loss analysis of mild steel in 0.5M H_2SO_4 at predetermined values of NNDT after 432 h exposure time

Sample	NNDT Concentration (%)	Weight Loss (mg)	Corrosion Rate (mm/y)	NNDT Efficiency (%)
A	0	3.365	17.926	0
B	0.25	0.327	1.4704	90.282
C	0.5	0.276	1.3377	91.798
D	0.75	2.581	12.326	23.299
E	1	1.093	4.5949	67.519
F	1.25	0.992	4.4966	70.52
G	1.5	0.812	3.4598	75.869

Table-2: Corrosion data for weight-loss analysis of mild steel in 0.5M HCl at predetermined values of NNDT after 432 h exposure time

Sample	NNDT Concentration (%)	Weight Loss (mg)	Corrosion Rate (mm/y)	NNDT Efficiency (%)
A	0	2.564	11.986	0
B	0.25	2.022	10.08	21.139
C	0.5	0.873	3.6795	65.952
D	0.75	0.94	3.6794	66.61
E	1	0.843	3.582	67.122
F	1.25	1.988	9.1189	22.465
G	1.5	2.362	11.254	7.878

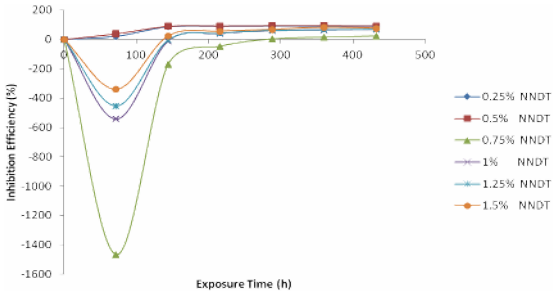

Fig. 2: Variation of NNDT efficiencies of sample (A-G) versus exposure time in 0.5 M H_2SO_4.

There are significant difference in values between Fig. 3 and 5, from 0.25% NNDT to 1.25% NNDT the % *IE* increased till a maximum value of 67%, after which there was a significant decrease in % *IE* from 1.25% - 1.5%NNDT. NNDT inhibition is assumed to be through the adsorption process resulting in the formation of an impenetrable protective film. The inhibitor influences the redox electrochemical process, affecting the cathodic regions of the steel surface through chemical interaction involving the protonated molecule in the acid solutions. The influence on the anodic sites involves donation of the electron-pair on the nitrogen atom of the non-ionized molecule. NNDT retards the hydrogen evolution and the metal degradation reactions synonymous with mixed type inhibiting compounds. Inhibitor adhesion onto the steel surface results from electrochemical interactions between the π-electrons of inhibitor molecules and d-orbital of valence electrons on the iron surface.

Observation of Tables 1 and 2 show that the %*IE* of NNDT is high at low concentrations of NNDT in H_2SO_4 compared with HCl acid. NNDT reacts more instantaneously in H_2SO_4 and more readily absorbs on to the steel. The %*IE* of NNDT indicated as the analogous contraction in corrosion rate which is significantly corresponds to the value of adsorbed inhibitors.

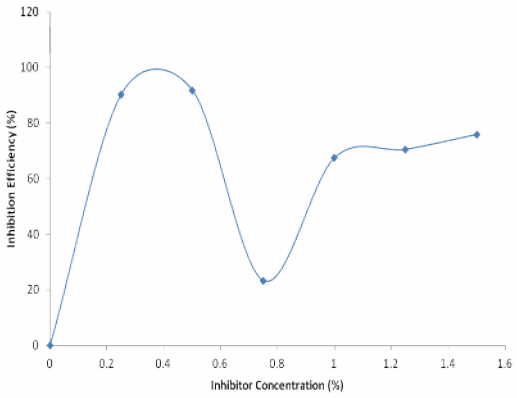

Fig. 3: Plot of percentage inhibition efficiency of NNDT versus NNDT concentration in 0.5 M H_2SO_4.

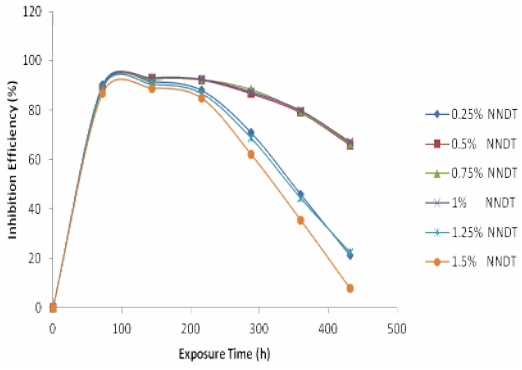

Fig. 4: Plot of inhibition efficiencies of sample (A - G) versus exposure time in 0.5 M HCl during the exposure period.

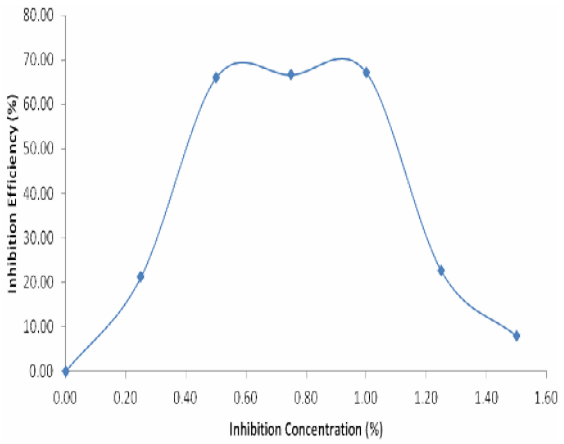

Fig. 5: Plot of NNDT Inhibition efficiency versus NNDT concentrations for weight loss in 0.5 M HCl.

Open Circuit Potential Measurement (OCP)

The OCP value of the steel samples was studied for 288 h in the test solutions are shown in Fig. 6 and 7. The figs depict the plot of OCP data against exposure time in 0.5 M H_2SO_4 and HCl solutions respectively, with and without the addition of predetermined concentrations of NNDT organic compound. The sample without NNDT inhibitor (0% NNDT) in the acid media shows significant degradation the steel samples as shown in the potential data. The values shifted significantly towards anodic potentials, attesting that metal dissolution is active in the absence of NNDT. This causes deterioration of the steel properties and subsequent evolution of corrosion products such as oxides in the solution. Potential data in Fig. 6 displays values inside the passive region (0.25% - 0.5% NNDT) *i.e.* there is appreciable corrosion inhibition as a result of the electrochemical action of NNDT corrosion process. The cations of the inhibitor molecules effectively counteract the electrochemical action of the corrosive species (SO_4^{2-} and Cl^-) in the test solution. Due to desorption and lateral repulsion at 0.75% NNDT the potential values decrease suddenly to greater anodic potentials. After 0.75% NNDT the potential values deviates steadily to passivation potentials till 1.5% NNDT. The value aligns with the inhibition efficiency obtained from the weight loss experiments.

Observation of corrosion potentials in Fig. 7 shows significant difference from Fig. 6 due to the differential mechanism of inhibition of NNDT in the solution. NNDT is unable to significantly influence the electrochemical reactions in the acid solution at 0.25% NNDT. The inhibitor molecules cannot inhibit the diffusion of corrosive anions, thus leading to failure of the steel samples, the potential values is highly anodic. With increase in NNDT concentration, the potentials decrease (0.5% - 1% NNDT) *i.e.* a significant deviation to passive potentials. This is due to the availability of more NNDT molecules for strong adsorption onto the steel surface resulting in corrosion inhibition. After 1% NNDT the potential decrease sharply (1.25% - 1.5% NNDT) as a result of desorption and lateral repulsion between the NNDT molecules. The deviation in potentials to passivation potentials in H_2SO_4 and HCl depicts the improvement of the corrosion resistance of the steel with NNDT addition due to physiochemical interaction of the NNDT molecules unto the steel surface.

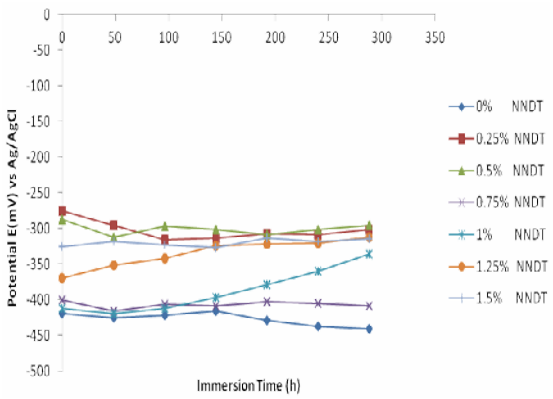

Fig. 6: Plot of OCP results versus exposure time for NNDT concentrations in 0.5 M H_2SO_4.

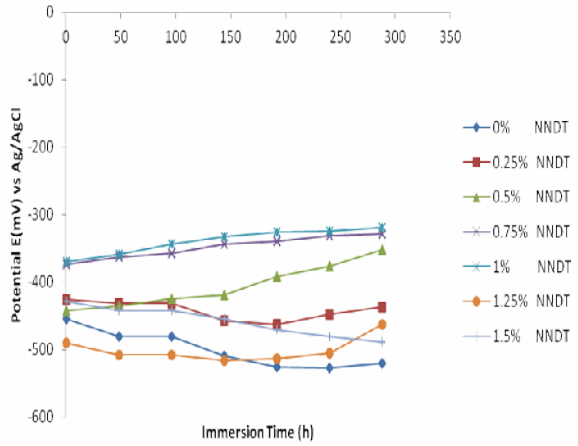

Fig. 7: Plot of OCP results versus exposure time for NNDT concentrations in 0.5 M HCl.

Polarization Studies

The electrochemical effect of NNDT on the corrosion polarization curves (anodic and cathodic)

for mild steel in the acid media was investigated. Observation of Fig. 8 depicts the polarization curves with and without NNDT addition at predetermined concentrations in 0.5 M H_2SO_4 while Fig. 9 shows the polarization curves in 0.5 M HCl solution. NNDT significantly influenced the corrosion behavior of the steel electrode in 0.5M H_2SO_4 solution from the lowest to the highest NNDT concentration excluding 0.75% NNDT whose result on % *IE* contrast others. Data on % *IE* in 0.5M HCl significantly differs from the data in 0.5M H_2SO_4 solution from observation of Table 3 and 4. Previous discussion on weight loss analysis confirms the inhibition performance of NNDT in H_2SO_4 is spontaneous from the lowest to the highest concentration due to the presence of a protective film which inhibits the transport of corrosive species. In HCl solution the %*IE* increased significantly after 0.25% NNDT concentration due to the presence of significant amount NNDT molecules to compete with and inhibit the electrochemical actions of the corrosive anions, block the active sites and form a protective film on the alloy surface in the acid solutions. After 1% NNDT the inhibition efficiency reduced rapidly due to the selective attributes NNDT in differing solutions and the formation of secondary precipitates. The corrosion potential in Fig. 9 deviates to potentials associated with cathodic inhibition with increase in NNDT concentration, thus protecting the steel inhibition of hydrogen evolution reactions through interaction between the NNDT and the oxidized metal surface which effectively seals it against further reaction. The cathodic process predominates over the anodic.

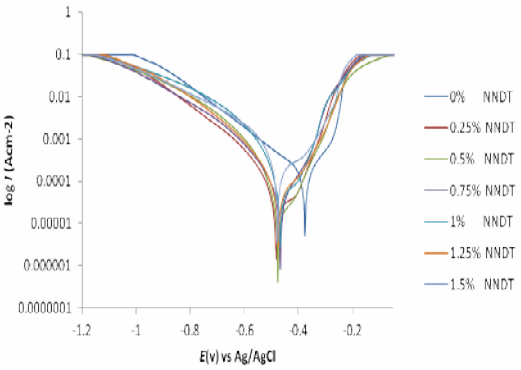

Fig. 8: Potentiodynamic polarization plot for mild steel in 0.5 M H_2SO_4 at predetermined concentrations of NNDT.

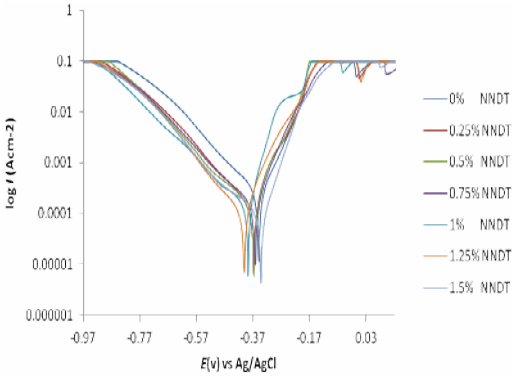

Fig. 9: Potentiodynamic polarization plot for mild steel in 0.5 M HCl at predetermined concentrations of NNDT.

Table-3: Potentiodynamic polarization resistance results for mild steel in 0.5 M H_2SO_4 at predetermined concentrations of NNDT.

Inhibitor Concentration (%)	Corrosion Rate (mm/yr)	% *IE*	R_p (Ω)	E_{corr}, Cal (V)	i_{corr} (A)	I_{corr} (A/cm²)	*bc* (V/dec)	*ba* (V/dec)
0	7.9	0	27.8	-0.376	1.12E-03	6.79E-04	0.091	0.336
0.25	0.87	88.94	152.95	-0.483	1.20E-04	7.27E-05	0.051	0.245
0.5	0.72	90.84	222.34	-0.477	1.00E-04	6.06E-05	0.067	0.216
0.75	4.22	46.57	65.88	-0.467	6.00E-04	3.64E-04	0.129	0.308
1	1.04	70.65	168.66	-0.468	1.50E-04	9.09E-05	0.106	0.129
1.25	0.96	66.32	130.48	-0.476	1.40E-04	8.48E-05	0.061	0.135
1.5	0.53	74.8	277.22	-0.476	8.00E-05	4.85E-05	0.07	0.188

Table-4: Potentiodynamic polarization resistance results for mild steel in 0.5 M HCl at predetermined concentrations of NNDT

Inhibitor Concentration (%)	Corrosion Rate (mm/yr)	% *IE*	R_p (Ω)	E_{corr}, Cal (V)	i_{corr} (A)	I_{corr} (A/cm²)	*bc* (V/dec)	*ba* (V/dec)
0	1.81	0	35.51	-0.347	2.57E-04	1.56E-04	0.032	0.061
0.25	1.37	24.36	24.59	-0.367	1.94E-04	1.18E-04	0.026	0.019
0.5	0.65	64.21	97.61	-0.365	9.23E-05	5.59E-05	0.067	0.03
0.75	0.51	71.68	100.33	-0.36	7.28E-05	4.41E-05	0.028	0.042
1	0.58	68.12	75.86	-0.388	8.16E-05	4.95E-05	0.035	0.024
1.25	1.31	27.84	28.11	-0.408	1.86E-04	1.12E-04	0.028	0.021
1.5	1.73	4.18	35.97	-0.343	2.46E-04	1.49E-04	0.027	0.082

Mechanism of Inhibition

NNDT being an organic compound consists of oxygen, sulfur, nitrogen atoms, and bonds in its molecules which aids its adsorption on the metal surface [20] and are strongly polar in nature, thus providing an electron rich reaction center. Immersion of mild steel in the test solutions results causes the aggregation of anions at the metal/solution interface in addition to Cl^- ions which causes the accumulation of excess negative charges on the metal surface. NNDT significantly affects influences the dynamics of the electrochemical reactions modifying the anodic dissolution of the metal in the acid solutions through adsorption. Adsorption is generally rapid and it occurs on the active sites enabling NNDT to dominate the redox reactions of the corrosion process. Due to the innate protonated hydrophilic amino and imino groups NNDT strongly adsorbs on the ionized steel surface, while their hydrophobic substituent (thiol) aligns the NNDT molecules during adsorption to form a protective film that shields the steel from the acid media. Thiol molecules form the protective film due to their strong attraction to metal and their ability to adapt due to hydrophobic interaction. The lone pair of electrons in NNDT molecules enables electron transfer from the NNDT to the metal through chemisorption mechanism [21]. NNDT performed more effectively in H_2SO_4 than in HCl based on corrosion rate and inhibition efficiency values from weight loss, open circuit potential and potentiodynamic polarization tests because chloride ions (Cl^-) ions are more aggressive than sulphate ions (SO_4^{2-}) on the steel, initiate general and pitting corrosion [22-26]. The small size and high reactivity of the Cl^- ions causes' rapid oxidation of the valence atoms of the steel leading the enhanced deterioration of the steel compared to SO_4^{2-} ions.

Scanning Electron Microscopy Analysis

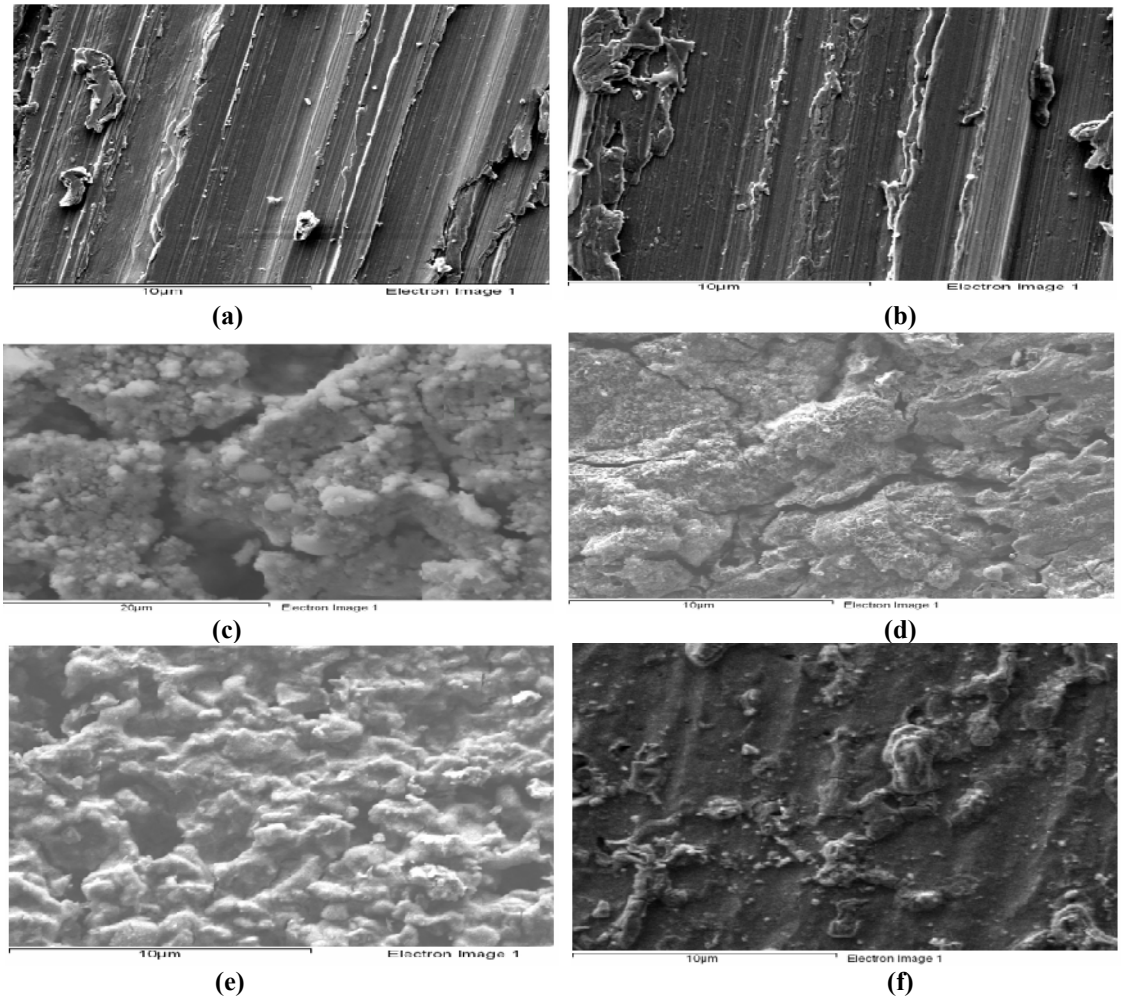

Fig. 10: Scanning electron micrographs of: a) Mild steel, b) Mild steel, c) Mild steel in 0.5 M HCl, d) Mild steel in 0.5 M HCl/NNDT, e) Mild steel in 0.5 M H_2SO_4, f) Mild steel in 0.5 M H2SO4/NNDT.

Scanning electron micrographs of mild steel topography before and after weight loss test in acid solutions and after 432 h exposure time at predetermined concentrations of NNDT are shown in Fig. 10(a–f). Figure 10a and b shows the mild steel before exposure, the serrated surfaces are the product of machining during preparation. Figure 10(c and e) shows the steel topography after 432 h of exposure in the acid media without NNDT, while Figure 10(d and f) shows the steel topography without NNDT. Without NNDT addition a coarse surface is observed in Fig. 10(c and e); a significant number of macro pits and deteriorated surface of the steel are conspicuous due to the corrosive actions of anionic species present in the solution. The micrograph in Fig. 10c shows a sample coated with chloride compounds from the solution and the admixture of chloride and sulphur in Fig. 10e. Their high electronegative property is responsible for their rapid diffusion during the electrochemical. This causes the electrolytic transport of Fe^{2+} into the solution and producing the observed topography with large macro pits. The scanning electron microscopy image of the steel sample with NNDT as shown in Fig. 10 (d and f) contrasts the control samples in both acids. The protective film depends on the percentage concentration of NNDT. The steel surface from the acid solutions with NNDT inhibitor is well protected, as the inhibitor molecules fully envelopes the entire the metal, resulting in a high degree of inhibition against corrosion.

XRD Analysis

The X-ray diffraction (XRD) patterns of the sample surfaces after exposure hours in the acid solutions in the presence and absence of NNDT are shown in Fig. 11a, 11b, 12a and 12b while the Identified Patterns List are shown in Tables 5, 6, 7 and 8 respectively. The peak values at 2θ for mild steel in without NNDT in H_2SO_4 and HCl media revealed the presence of phase compounds *i.e.* corrosion products on the steel surface. The peak values at 2θ = 36.9, 53.5, 40.2, 47.3, 64.3 and 74.8 for the steel after exposure in 0.5 M H_2SO_4 conforms to compounds such as manganese sulphide, manganese oxide, iron silicon oxide and iron oxides present on the surface quantitatively. Some of these phase compounds such as iron oxides are the products of corrosion. Manganese sulfide inclusions act as initiation sites leading to pitting and general corrosion [27–35]. The peak values at 2θ = 40.6° and 73.3° for mild steel after exposure in 0.5 M HCl conforms to iron oxide on the steel due to corrosion. Observation of the peak values (Fig.12b) on the surface of the steel after exposure in the 0.5 M H_2SO_4 solutions with NNDT showed the absence of chemical compounds/corrosion products associated with corrosion. Analysis of the steel surface from 0.5 M HCl with NNDT showed slight traces of iron oxide.

Table-5: Identified Patterns List for XRD analysis of mild steel in 0.5 M H_2SO_4 without NNDT.

Ref. Code	Score	Compound Name	Displacement [°2Th.]	Scale Factor	Chemical Formula
01-089-4088	35	Manganese Sulfide	-0.177	0.624	Mn S
00-008-0415	32	Graphite	0.079	0.195	C
01-075-0034	27	Iron Manganese Oxide	0.45	0.731	$Fe_3 Mn_3 O_8$
00-049-1447	27	Iron Oxide	-0.041	0.397	Fe O
00-052-1142	15	Iron Silicon Oxide	0.064	0.388	$Fe_{2.56} Si_{0.44} O_4$

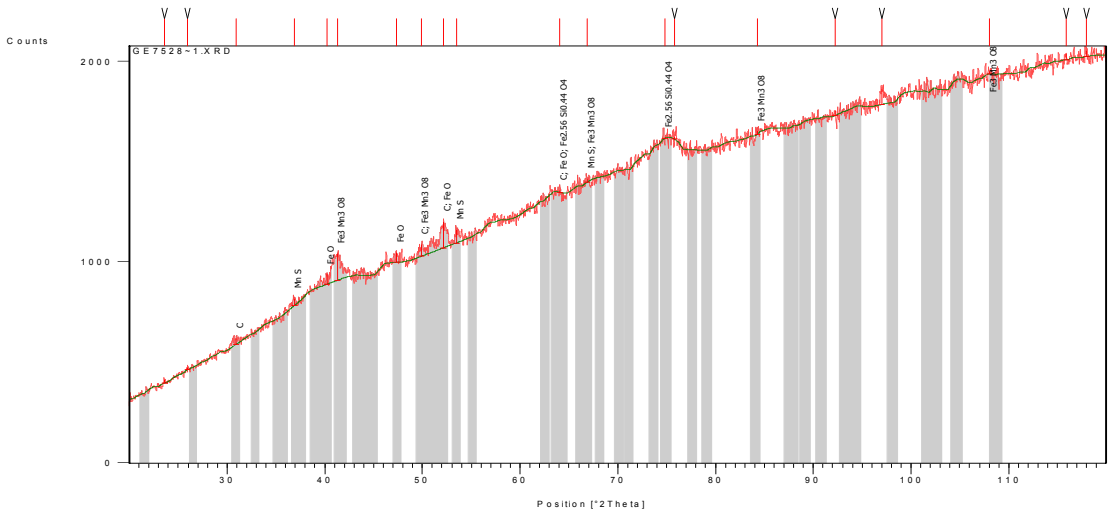

(a)

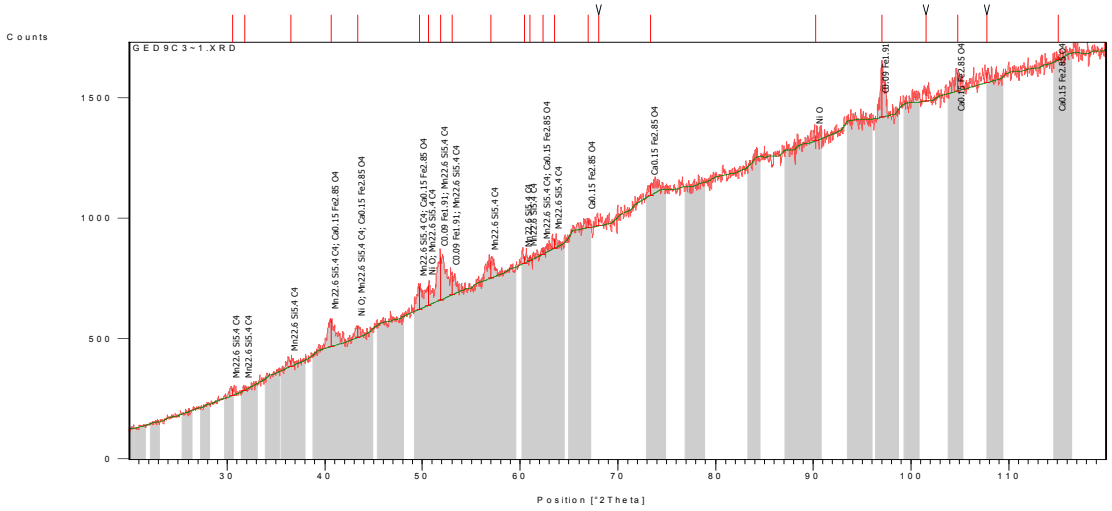

(b)

Fig. 11: X-Ray diffraction Patterns List for mild steel (a) in 0.5 M H_2SO_4 without NNDT (b) in 0.5 M HCl without NNDT.

Table-6: Identified Patterns List for XRD analysis of mild steel in 0.5 M HCl without NNDT.

Ref. Code	Score	Compound Name	Displacement [°2Th.]	Scale Factor	Chemical Formula
01-078-0429	45	Nickel Oxide	-0.28	0.224	Ni O
00-044-1292	36	Martensite	0.446	0.395	$C_{0.09}$ $Fe_{1.91}$
00-029-0887	31	Manganese Silicon Carbide	-0.065	0.422	$Mn_{22.6}$ $Si_{5.4}$ C_4
00-046-0291	21	Calcium Iron Oxide	0.038	0.31	$Ca_{0.15}$ $Fe_{2.85}$ O_4

Table-7: Identified Patterns List for XRD analysis of low carbon steel in 0.5 M H_2SO_4 with NNDT.

Ref. Code	Score	Compound Name	Displacement [°2Th.]	Scale Factor	Chemical Formula
01-087-0722	71	Iron	-0.639	1.011	Fe
01-089-6228	39	Iron Silicon Oxide	-0.52	0.204	$(Fe_{0.769}$ $Si_{0.231})$ $(Fe_{0.975}$ $Si_{0.025})_2$ O_4

Table-8: Identified Patterns List for XRD analysis of low carbon steel in 0.5M HCl with NNDT.

Ref. Code	Score	Compound Name	Displacement [°2Th.]	Scale Factor	Chemical Formula
01-087-0722	64	Iron	-0.426	0.999	Fe
01-073-0603	35	Hematite, syn	-0.582	0.006	Fe_2 O_3
00-033-0945	15	Austenitic steel	0.251	0.467	$Ni_{2.9}$ $Cr_{0.7}$ $Fe_{0.36}$
00-032-1361	26	Tin Sulfide	0.032	0.017	Sn S
00-065-3545	28	Manganese Phosphide	0.308	0.01	Mn_2 P
00-044-1291	30	martensite	0.016	0.091	$C_{0.08}$ $Fe_{1.92}$

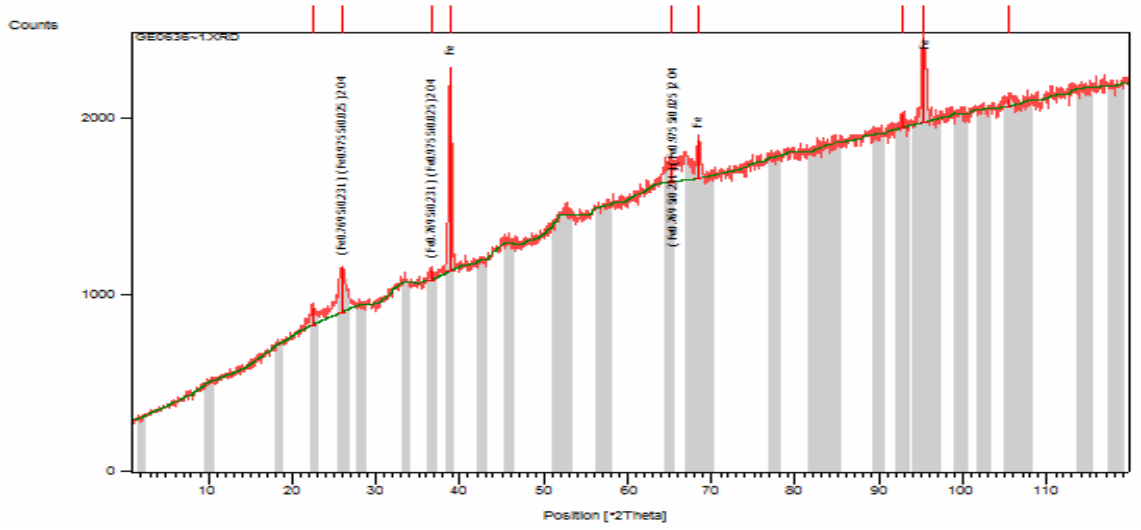

(a)

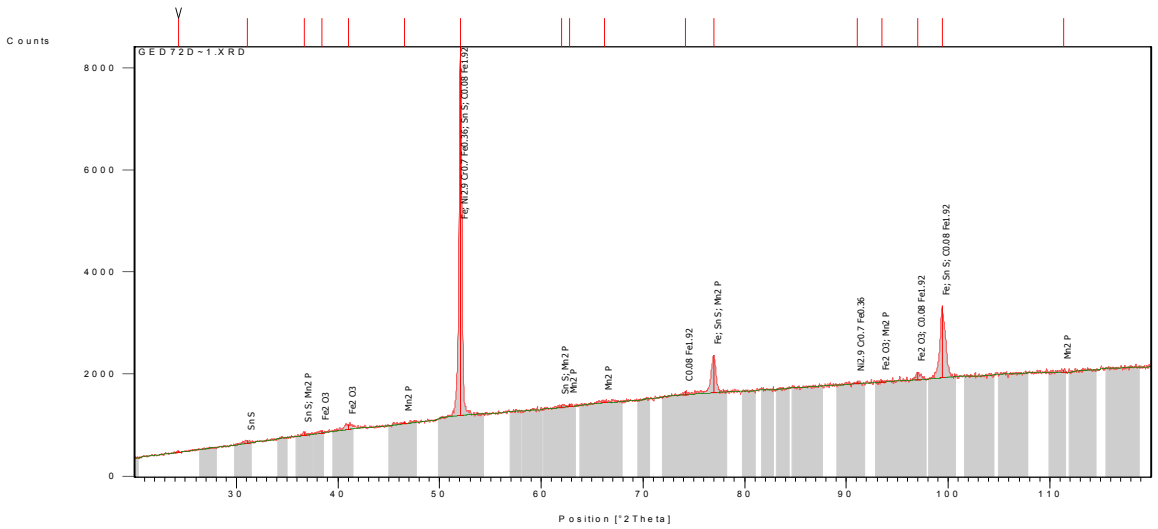

(b)

Fig. 12: X-Ray diffraction Patterns List for XRD analysis of low carbon steel (a) in 0.5 M H_2SO_4 with NNDT (b) in 0.5 M HCl with NNDT.

Table-9: Analysis of variance (ANOVA) for inhibition efficiency of NNDT inhibitor in 0.5 M H_2SO_4 (at 95% confidence level).

					Min. MSR at 95% confidence	
Source of Variation	**Sum of Squares**	**Degree of Freedom**	**Mean Square**	**Mean Square Ratio**	**Significance F**	**F (%)**
Inhibitor concentration	**571430.1**	**5**	**114286**	**11284.28**	**2.71**	**24.5**
Exposure Time	**1225410**	**4**	**306352.6**	**30248.38**	**2.87**	**69.96**
Residual	**202.56**	**20**	**10.13**			
Total	**1797043**	**29**				

Table-10: Analysis of variance (ANOVA) for inhibition efficiency of NNDT inhibitor in 0.5 M HCl (at 95% confidence level)

					Min. MSR at 95% confidence	
Source of Variation	**Sum of Squares**	**Degree of Freedom**	**Mean Square**	**Mean Square Ratio**	**Significance F**	**F (%)**
Inhibitor concentration	**1418.81**	**5**	**283.76**	**28.02**	**2.71**	**19.37**
Exposure Time	**4006.96**	**4**	**1001.74**	**98.91**	**2.87**	**75.06**
Residual	**202.56**	**20**	**10.13**			
Total	**5628.33**	**29**				

Statistical Analysis

Two-factor single level experimental ANOVA test (F-test) was applied to investigate the isolated and cumulative outcome of NNDT concentrations and exposure time on the %*IE* of NNDT in the corrosion of inhibition of mild steels in both acid solutions and to investigate the statistical connotation of the outcomes. The F-test was used to check the extent of modification within each of the samples relative to the extent of modification between the samples. The results using the ANOVA test is tabulated (Table 9 and 10) as displayed below.

Statistical analysis H_2SO_4 was studied at a confidence level of 95% *i.e.* the basis equivalent of $\alpha = 0.05$. The data on ANOVA shows both NNDT concentration and time of exposure time are statistically relevant on the %*IE* of NNDT with F-values of 11284.28 and 30248.38 each. These results are higher than significance factor at $\alpha = 0.05$ (*i.e.* probability equivalent). The statistical relevance of the NNDT concentration is 24.5% while the significance of the exposure time is 69.96%. The exposure time is numerically relevant than the NNDT concentration albeit both are important ideal premise affecting NNDT efficiency on mild corrosion. Based on the results obtained, NNDT concentration influences its %*IE* in the test solutions. The ANOVA results in 0.5 M HCl shows generally equal results. NNDT concentration and exposure time are statistically important with F-values of 28.02 and 98.91. These values are greater than the important determinant of $\alpha = 0.05$. The statistical importance of NNDT concentration is 19.37%, while the exposure time is 75.6% illustrating the overwhelming importance of exposure time on %*IE* of NNDT in HCl, however they affect the inhibition performance of NNDT in HCl media.

Conclusion

N, N-diphenylthiourea performed effectively with mixed results in the acid media. In H_2SO_4 acid NNDT showed excellent inhibiting tendency at low concentrations compared to HCl were there was a gradual increase in corrosion inhibition before decreasing. NNDT affects the mechanism of the redox electrochemical process within the test solutions inhibiting the anodic dissolution of the steel metal through adsorption. It showed cathodic inhibiting tendencies in H_2SO_4 and HCl at specific concentrations as shown in the values of corrosion potential due to interfacial reactions, where the inhibitor molecules are adsorbed via their functional groups and hetero-atoms onto the steel surface forming a protective layer. At a confidence level of 95% the ANOVA data show both NNDT concentration and exposure time to be numerically important on the inhibition efficiency of NNDT in both acids. SEM characterization revealed the absence of iron oxide and pits due to the evolution of a protective coating of NNDT on the steel surface. The protection of the film is dependent on the concentration of NNDT. Analysis of diffraction peaks for steel from 0.5 M HCl with NNDT showed trace quantities of iron oxides whereas the peaks from H_2SO_4 showed the complete absence of corrosion products.

Acknowledgement

The authors are grateful to the Department of Chemical, Metallurgical and Materials Engineering, Faculty of Engineering and the Built Environment, Tshwane University of Technology, Pretoria, South Africa for the facilitation of the research.

References

1. R. Döner, M. Solmaz, M. Özcan and G. Kardaş, Experimental and Theoretical Studies of thiazoles as Corrosion Inhibitors for Mild Steel in Sulphuric Acid Solution, *Corros. Sci*., **53**, 2902 (2011).
2. R. Solmaz, Investigation of the Inhibition Effect of 5-((E)-4-phenylbuta-1,3- dienylideneamino)-1,3,4-Thiadiazole-2-thiol Schiff Base on Mild Steel Corrosion in Hydrochloric Acid, *Corros. Sci*., **52**, 3321 (2010).
3. K. Parameswari, S. Chitra, A. Selvaraj, S. Brindha and M. Menaga, Investigation of Benzothiazole Derivatives as Corrosion Inhibitors for Mild Steel, *Port. Elect. Acta*., **30,** 126 (2012).
4. L. Dhouibi, E. Triki and A. Raharinaivo, The Application of Electrochemical Impedance Spectroscopy to Determine the Long-Term Effectiveness of Corrosion Inhibitors for Steel in Concrete, *Cement and Concrete Comp.,* **24**, 35 (2002).
5. O. Trocónis de Rincón, O. Pérez, E. Paredes, Y. Caldera, C. Urdaneta and I. Sandoval, Effect of Rebar Cleanliness and Repair Materials on Reinforcement Corrosion and Flexural Strength of Repaired Concrete Beams, *Cement Concrete Comp*., **24**, 139 (2002).
6. H. Liang, L. Li and N.D. Poor, Nitrite diffusivity in Calcium Nitrite-Admixed Hardened Concrete, *Cement Concrete Res.,* **33**, 139 (2003).
7. R. Cigna, G. Familiari, F. Gianetti and E. Proverbio, in: R. N. Swamy (Ed.), *Corrosion and Corrosion Protection of Steel in Concrete*, Sheffield, UK, **2**, 878 (1994).
8. *ISO* (Standard), (1986).
9. S. Muralidharan and S. V. K. Iyer, the Influence of N-heterocyclics on Corrosion Inhibition and Hydrogen Permeation through Mild Steel in Acidic Solutions, *Anti-Corr. Mets.* And *Mats.,* **44**, 100 (1997).
10. M. A. Quraishi, M. A. W. Khan and M. Ajmal, Oil and Gas Industry is Poorly Informed about Titanium Properties, *Anti-Corr. Mets. and Mats.,* **43**, 5 (1996).
11. O. X. Octavio, V. L. Natalya, N. Noel, C. P. Agustín, V. L. Irina, A. Escobedo-Morales and L. Claudia, Thiadiazoles as Corrosion Inhibitors for Carbon Steel in H_2SO_4 Solutions, *Int. J. of Elect. Sci.,* **8**, 735 (2013).
12. F. Zucchi, G. Trabanelli, G. Brunoro, C. Monticelli and G. Rochini, Corrosion Inhibition of Carbon and Low Alloy Steels in Sulphuric Acid Solutions by 2-Mercaptopyrimidine Derivatives, *Mats. and Corr*, **44**, 264 (1993).
13. M. M. Osman, E. Khamis and A. Michael, The Influence of Triazolidines on the Acidic Corrosion of Steel, *Corr. Prev. and Control.,* **41**, 60 (1994).
14. S. C. Bilgic and N. Calıskan, An Investigation of Some Schiff Bases as Corrosion Inhibitors for Austenitic Chromium-Nickel Steel in H_2SO_4, *J. of Appl. Electrochem.,* **31**, 79 (2001).
15. M. Quraishi and R. Sardar, Dithiazolidines—A New Class of Heterocyclic Inhibitors for Prevention of Mild Steel Corrosion in Hydrochloric Acid Solution, *Corrosion*, **58**, 103 (2002).
16. M. A. Quraishi and D. Jamal, Dianils as New and Effective Corrosion Inhibitors for Mild Steel in Acidic Solutions, *Mats. Chem. and Phys.,* **78**, 608 (2003).

17. N. Jin-Yan, S. Yun-Sen, Y. Qiang, W. Zhao-di, Inhibition Effect of N,N′-Diphenyl Thiourea on Corrosion of Q235 Steel in Acid Medium and Synergistic Effect with Sodium Dodecyl Sulfate, *Corr. Sci. and Prot. Tech*., **5** (2011).
18. S. Divakara Shetty, Prakash Shetty, and H. V. Sudhaker Nayak, Inhibition of Mild Steel Corrosion in Acid Media by n-(2-thiophenyl)-n/-phenyl thiourea, *J. Chil. Chem. Soc*., **51**, 849 (2006).
19. N. Jin-Yan, S. Yun-Sen, Y. Qiang, W. Zhao-di, Contrast Study on the Inhibitive Effect of N,N-diphenyl Thiourea and Thiourea on the Corrosion of A_3 Steel in Acid Medium, *Surf. Tech*. **1** (2010).
20. A. G. Gad and H. M. Tamous, Structural Investigation of Pyrazole Derivatives as Corrosion Inhibitors for Delta Steel in Acid Chloride Solutions, *J. of Appl. Electrochem.,* **20**, 488 (1990).
21. M. A.Quraishi and H. K. Sharma, 4-Amino-3-butyl-5-mercapto-1,2,4-triazole: a New Corrosion Inhibitor for Mild Steel in Sulphuric Acid, *Mats. Chem. and Phys.,* **78**, 18 (2002).
22. Q. Yang and J. L. Luo, Effects of Hydrogen and Tensile Stress on the Breakdown of Passive Films on Type 304 Stainless Steel, *Electrochim. Acta*., **46**, 851 (2001).
23. E. A. Abd El Meguid, N. A. Mahmoud and S. S. Abd El Rehim, The Effect of Some Sulphur Compounds on the Pitting Corrosion of Type 304 Stainless Steel, *Mater. Chem. Phys*., **63**, 67 (2000).
24. S. K. Phanis, A. K. Satpati, K. P. Muthe and J. C. Vyas and R. I. Sundaresan, Comparison of Rolled and Heat Treated SS304 in Chloride Solution using Electrochemical and XPS Techniques, *Corros. Sci*., **45**, 2467 (2003).
25. M. A. Ameer, M. A., Fekry and F. El-Taib Heakel, Electrochemical Behaviour of Passive Films on Molybdenum-Containing Austenitic Stainless Steels in Aqueous Solutions, *Electrochim. Acta.,* **50**, 43 (2004)
26. S. S. El-egamy and W. A. Badway, Passivity and Passivity Breakdown of 304 Stainless Steel in Alkaline Sodium Sulphate Solutions, *J. Appl. Electrochem*., **34**, 1153 (2004).
27. J. E. Castle and R. Ke, Studies by Auger Spectroscopy of Pit Initiation at the Site of Inclusions in Stainless Steel, *Corros. Sci.,* **30**, 409 (1990).
28. M. A. Baker and J. E. Castle, Growth Process of Protective Oxides Formed on Type 304 and 430 Stainless Steels at 1273 k, *Corros. Sci.,* **33**, 1295 (1992).
29. R. Ke and R. Alkire, Surface Analysis of Corrosion Pits Initiated at MnS Inclusions in 304 Stainless Steel, *J. of the Elect. Soc.*, **139**, 1573 (1992).
30. M. A. Baker and J. E. Castle, The Initiation of Pitting Corrosion at MnS Inclusions, *Corros. Sci*., **34**, 667 (1993).
31. R. Ke and R. Alkire, Initiation of Corrosion Pits at Inclusions on 304 Stainless Steel, *J. of the Electrochem. Soc.,* **142**, 4056 (1995).
32. G. S. Frankel, Pitting Corrosion of Metals: A Review of the Critical Factors, *J. of the Electrochem. Soc.,* **145**, 2186 (1998).
33. H. Krawiec, V. Vignal, O. Heintz, R. Oltra and J. M. Olive, Influence of the Chemical Dissolution of MnS Inclusions on the Electrochemical Behavior of Stainless Steels, *J. of the Electrochem. Soc*., **152**, B213 (2005).
34. T. L. Wijesinghe and D. J. Blackwood, Real Time Pit Initiation Studies on Stainless Steels: The Effect of Sulphide Inclusions,'' *Corros. Sci.*, **49**, 1755 (2007).
35. G. S. Eklund, Initiation of Pitting at Sulfide Inclusions in Stainless Steel, *J. of the Electrochem. Soc.,* **121**, 467 (1974).